AGU100 ADVANCING EARTH AND SPACE SCIENCE

JGR

Journal of Geophysical Research: Atmospheres

RESEARCH ARTICLE
10.1029/2017JD027427

Key Points:
- We present a new data set of rain $\delta^{18}O$ and δD of Indian Summer Monsoon
- Rain $\delta^{18}O$ over central and northern India is influenced by varying moisture transport pathways
- Isotope-enabled GCM captures intraseasonal variations in rain $\delta^{18}O$

Supporting Information:
- Supporting Information S1
- Data Set S1

Correspondence to:
M. Midhun,
midhun.ndr@gmail.com;
midhun@cusat.ac.in

Citation:
Midhun, M., Lekshmy, P. R., Ramesh, R., Yoshimura, K., Sandeep, K. K., Kumar, S., et al. (2018). The effect of monsoon circulation on the stable isotopic composition of rainfall. *Journal of Geophysical Research: Atmospheres*, *123*, 5205–5221. https://doi.org/10.1029/2017JD027427

Received 8 JUL 2017
Accepted 22 APR 2018
Accepted article online 1 MAY 2018
Published online 29 MAY 2018

The Effect of Monsoon Circulation on the Stable Isotopic Composition of Rainfall

M. Midhun[1,2,3], P. R. Lekshmy[1,2], R. Ramesh[1,3,4], Kei Yoshimura[5,6], K. K. Sandeep[7], Samresh Kumar[8], Rajiv Sinha[9], Ashutosh Singh[10], and Shalivahan Srivastava[11]

[1]Geosciences Division, Physical Research Laboratory, Ahmedabad, India, [2]Department of Atmospheric Science, Cochin University of Science and Technology, Kochi, India, [3]School of Earth and Planetary Sciences, National Institute of Science Education and Research, Khordha, India, [4]Deceased 2 April 2018, [5]Atmosphere and Ocean Research Institute, The University of Tokyo, Kashiwa, Japan, [6]Institute of Industrial Science, The University of Tokyo, Komaba, Japan, [7]Centre for Atmospheric Sciences, Indian Institute of Technology, Delhi, India, [8]Department of Earth and Environmental Sciences, Indian Institute of Science Education and Research, Bhopal, India, [9]Department of Earth Sciences, Indian Institute of Technology, Kanpur, India, [10]Department of Geology, Delhi University, New Delhi, India, [11]Indian Institute of Technology (Indian School of Mines), Dhanbad, India

Abstract Understanding the factors that control the variability of oxygen isotopic ratios ($\delta^{18}O$) of Indian Summer Monsoon (ISM) rainfall ($\delta^{18}O_p$) is of vital importance for the interpretation of $\delta^{18}O_p$ derived from climate proxies (e.g., speleothem and tree ring cellulose) of this region. Here we demonstrate the importance of moisture transport pathways on spatiotemporal variations of ISM $\delta^{18}O_p$ using a new set of daily observations from central and northern India and previously reported data aided by simulations from an isotope-enabled General Circulation Model. ^{18}O-depleted rain events are characterized by a higher number of air parcel back trajectories through the Bay of Bengal branch of moisture transport, while those through the Arabian Sea branch are associated with ^{18}O enriched rain events. This effect is observed on intraseasonal to interannual timescales in the long-term observations at New Delhi as well. Thus, the shift in moisture transport regimes must be considered when interpreting $\delta\ ^{18}O_p$ from climate proxies of the ISM region.

1. Introduction

The Indian Summer Monsoon (ISM), rainfall associated with the seasonal northward migration of the Intertropical Convergence Zone during the boreal summer, is the major source of freshwater to the Indian subcontinent. Extreme variations in ISM (droughts and floods) have a strong effect on the agriculture and economy of the countries in this region (Gadgil & Gadgil, 2006). Hence, accurate prediction and future projection of ISM have great societal importance, yet it remains an unsolved scientific question. Paleoclimate studies can provide better insights into the natural variability of monsoons on longer timescales as well as ISM's response to different climate forcings (e.g., CO_2 variations and insolation changes) and teleconnections (e.g., Berkelhammer et al., 2013; Sinha et al., 2015). The abundant availability of stable oxygen isotope proxies in speleothems, tree rings, and ice cores offers a huge potential to investigate past ISM variability and its mechanisms. However, understanding the processes that control rainfall isotope variability in ISM is a prerequisite to the effective utilization of such isotope proxies.

Variability in the ^{18}O content of tropical rainfall proxies is classically interpreted as the variability of past rainfall (the amount effect; Dansgaard, 1964). The amount effect is the observed negative correlation between the monthly rainfall and its weighted mean ^{18}O content. Though this relation is quite robust over tropical island stations, it shows a large scatter over continents (Kurita, 2013; Lekshmy et al., 2015). Thus, the role of local and remote meteorological factors that control $\delta^{18}O$ of precipitation ($\delta^{18}O_p$) needs to be explored for a precise interpretation of ^{18}O-based continental monsoon proxies.

In the limited observations over the ISM region, the amount effect shows a large spatial variation (Breitenbach et al., 2010; Laskar et al., 2015; Lekshmy et al., 2014, 2014; Midhun & Ramesh, 2016; Yadava et al., 2007). From the three long-term stations in India (New Delhi, Mumbai, and Kozhikode) only New Delhi shows a significant amount effect during ISM on the monthly timescale. On the interannual timescale, a significant amount effect is observed at New Delhi and Kozhikode. Among these, only New Delhi shows a significant amount effect during ISM on a monthly timescale. Simulations of ISM from multiple isotope-enabled General Circulation Models (GCMs) also show a noisy pattern in the simulated amount effect over

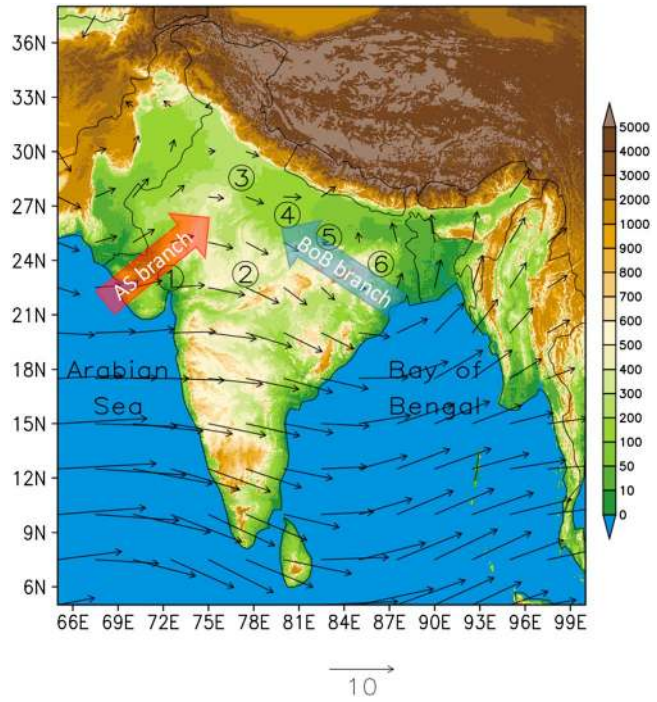

Figure 1. Topography of the ISM region (legend on the right: shades represent heights above mean sea level in meters) and climatological wind vectors at 850-hPa level during June to September (arrows, unit: m/s, source: NCEP). Sampling stations represented by circles are (1) Ahmedabad, (2) Bhopal, (3) New Delhi, (4) Kanpur, (5) Varanasi, and (6) Dhanbad. Two moisture transport pathways (AS branch and BoB branch) are also highlighted.

the continent but a strong, consistent amount effect over the ocean (Midhun & Ramesh, 2016). This suggests that the controlling factors of the rainfall-^{18}O relation over ocean and continent are quite different. The extent of organized convection (Kurita, 2013; Lekshmy et al., 2014) is the major cause of high depletion in $^{18}O_p$ over the ocean leading to a stronger amount effect. On the other hand, over the continent, $\delta^{18}O_p$ is determined by two factors: (i) local processes (local convection, rain reevaporation, etc.) and (ii) $\delta^{18}O$ of advected vapor (Lee et al., 2012; Lee & Fung, 2008). Hence, the strength of the amount effect will be determined by the dominance of either of these competing factors. If local convection dominates in $\delta^{18}O_p$ variability, it could lead to a strong amount effect. Similarly, rain reevaporation can also enhance the amount effect in the areas of low humidity (Lee et al., 2012; Midhun & Ramesh, 2016). The local amount effect is likely to be weak or absent in the areas where $\delta^{18}O$ of advected vapor primarily governs $\delta^{18}O_p$. In such regions, moisture advection pathways and the processes along the moisture pathways play a major role in $\delta^{18}O_p$ variability. Two distinct moisture advection pathways (Figure 1) are observed in the ISM region over central and northern India, the southwesterly branch from the Arabian Sea (the AS branch), and the easterly/southeasterly branch from the Bay of Bengal (the BoB branch). Mixing of vapor from these two branches plays a major role in determining the $\delta^{18}O_p$ at New Delhi (Saikat Sengupta & Sarkar, 2006). Recently, Sinha et al. (2015) reported a higher depletion in $^{18}O_p$ associated with enhanced moisture transport from the BoB branch. Therefore, it is important to quantify the effect of lower tropospheric circulation (and thereby moisture transport pathways) on the ISM $\delta^{18}O_p$ variability.

Here we investigate the spatiotemporal variations of daily $\delta^{18}O_p$ and δD_p (stable hydrogen isotope ratio of precipitation) during ISM 2013 over the central and northern Indian regions, together with the previously existing $\delta^{18}O_p$ data from this region. The main objectives are (i) to identify the role of lower tropospheric circulation on the spatial pattern of ISM $\delta^{18}O_p$ and (ii) to explore the local and remote meteorological factors that control temporal variations in ISM $\delta^{18}O_p$ on different timescales (intraseasonal to interannual).

2. Data and Methodology

2.1. Sampling

During the ISM season (June–September [JJAS]) 2013, daily rainwater samples (n = 216) were collected from six stations across northern and central India (Figure 1) whenever it rained. Most of the precipitation over the Indo-Gangetic plain originates from rainfall associated with the northwestward movement of monsoon depressions that form over the northern BoB (characterized by the BoB branch; Sikka, 1977). Four rain sampling stations (Dhanbad, Varanasi, Kanpur, and Delhi) were established along this transect. Rainwater samples were also collected from two stations from western and central India (Ahmedabad and Bhopal) which are mainly influenced by the AS branch of moisture transport. Here we use the terms "AS branch" and "BoB branch" to indicate the moisture transport pathways (Figure 1), which does not mean that the sources of moisture are the respective oceanic regions. Moisture sources may include evapotranspiration and raindrop reevaporation in addition to the oceanic evaporation.

2.2. Isotopic Analysis

The stable isotopic analysis was done using a continuous flow Thermo Delta-V-Plus isotope ratio mass spectrometer at the Physical Research Laboratory, Ahmedabad, India. The CO_2-H_2O equilibration technique (Epstein & Mayeda, 1953) using GasBench-II is adopted for $\delta^{18}O$ measurements. Similarly, H_2O-H_2 equilibration in the presence of a platinum catalyst (Horita, 1988) is adopted for δD measurements. All

measurements were carried out using an intermediate laboratory standard Narmada river water and finally reported in Vienna Standard Mean Ocean Water scale. We participated in the fourth interlaboratory comparison exercise for δD and $\delta^{18}O$ analysis of water samples (WICO2011), and our measurements are in good agreement with the IAEA consensus values (Ahmad et al., 2012). The precision of our measurements (1σ) was better than 0.1‰ for $\delta^{18}O$ and 1‰ for δD. The error associated with the calculation of *d*-excess ($\delta D - 8\delta^{18}O$) was less than 1.3‰.

2.3. Back Trajectory Modeling

Ten-day back trajectories of air parcels reaching 1,000; 1,500; and 2,000 m above the sampling stations were calculated to check the role of moisture sources and processes along parcel trajectories on $\delta^{18}O_p$ variability. We selected the heights because of maximum moisture transport as well as moisture convergence that occur here. We used the HYbrid Single-Particle Lagrangian Integrated Trajectory (HYSPLIT; Draxler & Rolph, 2003) model with 2.5° × 2.5° gridded data from the National Center for Environmental Prediction (NCEP) reanalysis-1 (Kalnay et al., 1996) as the input meteorological fields. Since each of the samples represents the daily accumulated rainfall, we initiated trajectories four times a day, resulting in a total of 12 (four times at three heights) trajectories per each rain sample. We estimated the trajectory density at each grid point at a resolution of 0.5 × 0.5° by counting the number of trajectories that crossed each grid point. We have interpolated 0.25° × 0.25° 3-hourly Tropical Rainfall Measuring Mission (TRMM) 3B42 (Goddard Earth Sciences Data and Information Services Center, 2016) rainfall along the trajectory to study the role of rainfall along the trajectory on $\delta^{18}O_p$. We used TRMM data because precipitation fields in the NCEP reanalysis are from the forecast field, not from the analyzed field, whereas TRMM rainfall data rely on actual satellite observations. TRMM has some dry bias over the Western Ghat region during ISM (Mitra et al., 2013), but it is the only observational data set available (Mitra et al., 2013) at 3-hourly resolution covering both land and ocean during the study period. Monsoon trajectories (JJAS months) reaching the Global Networks of Isotopes in Precipitation (GNIP) station New Delhi during the period 1961 to 2009 were also calculated to understand the role of circulation on the interannual variability of $\delta^{18}O_p$. For this, we limited our analysis to one trajectory per rainy day (days with rainfall >1 mm of rain, $n = 1{,}743$). Apart from the NCEP reanalysis, we have also carried out HYSPLIT trajectory analysis using simulations from an isotope-enabled GCM (Yoshimura et al., 2008).

Rainfall events at each station were classified into three categories: (i) ^{18}O-enriched events (events with $\delta^{18}O_p > (\mu + 0.5\sigma)$, where μ and σ are the mean and standard deviation of $\delta^{18}O_p$ at each station), (ii) ^{18}O median events (events with $(\mu - 0.5\sigma) < \delta^{18}O_p < (\mu + 0.5\sigma)$), and (iii) ^{18}O-depleted events (events with $\delta^{18}O_p < (\mu - 0.5\sigma)$). Results are consistent with the selection of criteria of $\mu \pm \sigma$ also, but $\mu \pm 0.5\sigma$ is used to increase the number of events in depleted and enriched categories. We calculated the composite trajectory density for each category for further analysis. Since $\delta^{18}O_p$ and δD are highly correlated ($r^2 > 0.98$) only $\delta^{18}O_p$ is used in this analysis, but the conclusions are valid for δD as well.

2.4. Moisture Flux Calculation

Vertically integrated moisture flux (*Q*) was calculated, on daily, monthly, and interannual timescales, from the NCEP reanalysis using the following equations,

$$Q_v = \frac{1}{g}\int_{P_t}^{P_s} qv\,dp \tag{1}$$

Where Q_u is the zonal components of *Q*, *g* is the acceleration due to gravity, *q* is the specific humidity, *u* and *v* are the zonal and meridional component of the wind, and P_t and P_s represent the 300 hPa and surface pressure, respectively.

2.5. Model Description

An ISM simulation from IsoGSM, the isotope-enabled version of NCEP's Global Spectral Model (Yoshimura et al., 2008), is validated in the present study. We used the following model outputs for all atmospheric fields: (i) with a 6-hour resolution for the year 2013 and (ii) with monthly averages for the years 1980 to 2007. The spatial resolution of the model is 1.9° latitude × 1.8° longitude. The model is forced with observed sea surface temperatures, while the large-scale wind fields and temperature are constrained with the observations (NCEP reanalysis II; Kanamitsu et al., 2002) using the spectral nudging technique (Yoshimura & Kanamitsu, 2008). The nudging technique helps in simulating a more realistic atmospheric circulation and thereby improves the ISM

Table 1
Rainfall and Its Isotopic Characteristics at Each Station

Station name and coordinates	Number of samples	Rainfall in 2013 (mm) Climatology[a] is given in the bracket	JJAS rain weighted mean		LMWL[b]			Amount effect[c]	
			$\delta^{18}O_p$ (‰)	d-excess (‰)	Slope	Intercept	R^2	Slope (‰/mm)	R^2
Ahmedabad 23.04°N 72.49°E	49	1,249 (624 ± 231)	−5	13.5	7.8 ± 0.2	11.5 ± 0.7	0.98	−0.05 ± 0.01	0.23
Bhopal 23.25°N 77.45°E	58	960 (967 ± 200)	−6	10.8	7.7 ± 0.1	8.2 ± 0.6	0.99	−0.05 ± 0.02	0.07
New Delhi 28.55°N 77.19°E	26	530 (612 ± 195)	−8.7	12.2	7.6 ± 0.1	7.8 ± 1.2	0.99	−0.08 ± 0.03	0.19
Kanpur 26.51°N 80.23°E	28	989 (694 ± 156)	−8.2	13	8.0 ± 0.2	11.7 ± 1.6	0.98	−0.02 ± 0.02	0.05
Varanasi 25.29°N 82.99°E	38	726 (761 ± 218)	−9.7	11.8	7.6 ± 0.1	7.4 ± 1.2	0.99	−0.09 ± 0.03	0.15
Dhanbad 23.81°N 86.44°E	61	656 (967 ± 172)	−8.9	11.3	7.6 ± 0.1	7.2 ± 0.9	0.99	−0.07 ± 0.03	0.07

Note. JJAS = June–September.
[a]Climatological mean and standard deviation are calculated at the nearest grid in the CRU.TS3.21 data set during 1980–2010 CE (Harris et al., 2014). [b]LMWL is the local meteoric water line: δD_p = slope × $\delta^{18}O_p$ + intercept. [c]Amount effect: $\delta^{18}O_p$ = slope × rainfall + constant.

simulation (Midhun & Ramesh, 2016). Reference is made to Yoshimura et al. (2008) for further details about IsoGSM and model setup.

2.6. IsoMAP

$\delta^{18}O_p$ observations exist over many stations across India, but their temporal coverage is not uniform. Data are available for only a few years at most of the stations making it difficult to obtain a climatological mean spatial distribution of ISM $\delta^{18}O_p$. To overcome this, we used a web-based geoinformation system called IsoMAP (http://isomap.org). IsoMAP uses a hybrid method that involves regression and geostatistical interpolation. First, a regression model is constructed to predict $\delta^{18}O_p$ from meteorological and/or geographical parameters (in this study, elevation and latitude). All observations during the ISM season available at the GNIP database for the period 1961 to 2005 are used to construct the regression model. Then a regression model is applied on a high-resolution data set of topography to predict $\delta^{18}O_p$. Model residuals at each of the GNIP stations are then spatially interpolated using a kriging method and then added to the prediction of the regression model to obtain the climatological spatial means of $\delta^{18}O_p$ (Bowen, 2010). IsoMAP-predicted climatologies are used to study the spatial distribution $\delta^{18}O_p$ during ISM and to check whether the 2013 observations are consistent with the climatology.

2.7. Correlation Analysis

To assess the linear relationship between $\delta^{18}O_p$ and other climate parameters, we used the Pearson correlation coefficient. The significance is calculated using the method proposed by Ebisuzaki (1997) to avoid the effect of autocorrelation. In this method, 10,000 random variables are generated that have an identical frequency spectrum to the original time series but with different phases in each frequency. All these random time variables (and the original time series) are then correlated with the time series of the other variables. Then the significance level is calculated as the probability of the correlation coefficient obtained using original time series vis-a-vis the random time series. A significant level of $P < 0.05$ (two-tailed) is fixed to reject the null hypothesis.

3. Results and Discussion

3.1. Rainfall and Isotopic Characteristics

ISM rainfall over India was normal in 2013 (~6% higher compared to the long-term climatology, but the standard deviation is 10%; Pai & Bhan, 2014). Table 1 shows the JJAS seasonal total rainfall (i.e., ISM) and its $\delta^{18}O_p$ at each station. Rainfall at individual stations was either higher or lower relative to the local climatological mean (Table 1). However, the JJAS rain-weighted $\delta^{18}O_p$ for 2013 at each station was relatively more negative compared to both the previously reported values at its nearest GNIP station, and the climatological ISM $\delta^{18}O_p$ predicted by IsoMAP (supporting information Table S1 and Figure 4c). This negative anomaly is possibly due to anomalously high regional/upstream convection and the associated rainfall (Figure 4a). The short time spans of previous GNIP observations and the errors associated with the IsoMAP estimation (1σ ranging from 1‰ to 1.5‰), however, restrict us from making any definite conclusion about the interannual variation of

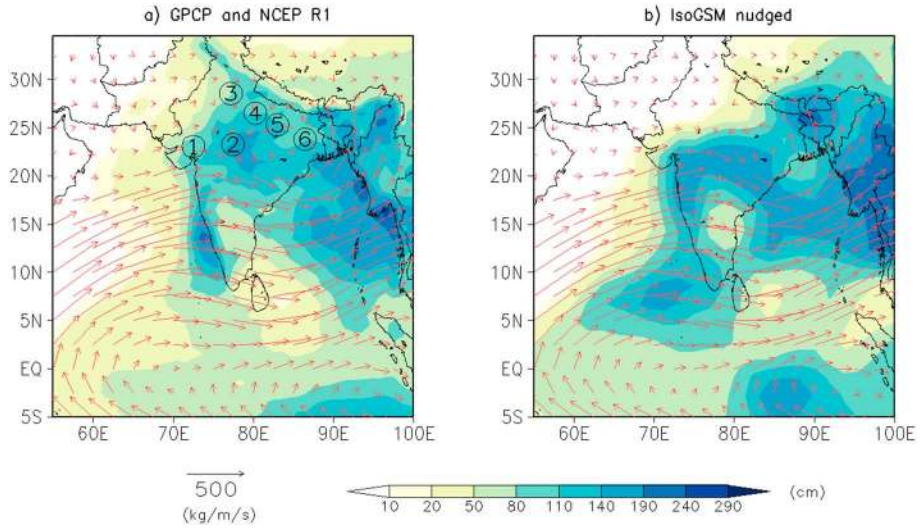

Figure 2. (a) Spatial pattern of total rainfall (shaded, source: GPCP) and the mean vertically integrated moisture flux (vectors, source: NCEP) during June–September 2013. Numbers indicate sampling stations. (b) Same as figure (a) but from the IsoGSM simulation for ISM 2013. Refer to Figure 1 for station names. GPCP = Global Precipitation Climatology Project; NCEP = National Center for Environmental Prediction; IsoGSM = Isotope-enabled Global Spectral Model; ISM = Indian Summer Monsoon.

$\delta^{18}O_p$. The slope of the local meteoric water line during 2013 at each site varied from 7.6 to 8.0, and the intercept varied from 7.2‰ to 11.7‰, comparable to the previously reported values over this region (Deshpande et al., 2010; Kumar et al., 2010; Sengupta & Sarkar, 2006).

3.2. Amount Effect:

A significant amount effect on the daily timescale is observed at five stations but explains only ~7% to 23% of the observed variance of daily $\delta^{18}O_p$ (Table 1). The most significant amount effect is observed at Ahmedabad ($r^2 = 0.23$), followed by New Delhi ($r^2 = 0.19$) and Varanasi ($r^2 = 0.15$); all r^2 values are significant at 0.05 level or better. The remaining three stations show a very weak or insignificant amount effect on the daily scale. We also checked the effect of the nonnormality of daily rainfall data on the calculated amount effect by linear regression after transforming it to a normal distribution (van Albada & Robinson, 2007). After the transformation, the amount effect improved at all six stations and explained 10% to 32% of the $\delta^{18}O_p$ variance (supporting information Figures SF3 and SF4).

3.3. Comparison With IsoGSM Simulations

The IsoGSM simulation of ISM 2013 is evaluated using the new data set (Figures 2–4 and Table 2). Figure 2 compares the spatial pattern of rainfall and moisture transport vectors between the nudged simulation of IsoGSM and observations. The linear correlation coefficient between the simulated and observed spatial distribution of rainfall that is 0.81 (pattern correlation) for the area shown in Figure 2 (daily rainfall data from the Global Precipitation Climatology Project (GPCP, Adler et al., 2003) is interpolated onto the model grid for calculating the correlation coefficient). However, IsoGSM underestimates the northwestern limit of ISM rainfall, especially in the region beyond Kanpur. This is a major drawback associated with most of the GCMs (e.g.,Midhun & Ramesh, 2016). The model captures the anomalous rainfall over the central Indian region, which is one of the major features of ISM 2013 (Figures 2 and 4). The spatial pattern of observed and model-predicted anomalies in ISM $\delta^{18}O_p$ and rainfall suggests the possible influence of upstream rainfall on $\delta^{18}O_p$ (mainly due to the anomalous rainfall over central India). This aspect is further explored using HYSPLIT back trajectory analysis and discussed in section 3.4.

Table 2
Correlations of Modeled (IsoGSM) Rainfall With Measured Rainfall, and Modeled $\delta^{18}O_p$ With Observed $\delta^{18}O_p$

	Correlation coefficient (*r*)	
Station	Rainfall	$\delta^{18}O_p$
Ahmedabad	0.39*	0.68*
Bhopal	0.09	0.45*
Delhi	0.03	0.73
Kanpur	0.08	0.50*
Varanasi	0.06	0.61*
Dhanbad	0.30*	0.58*

Note. IsoGSM = IsoGSM = Isotope-enabled Global Spectral Model.
*$P < 0.05$.

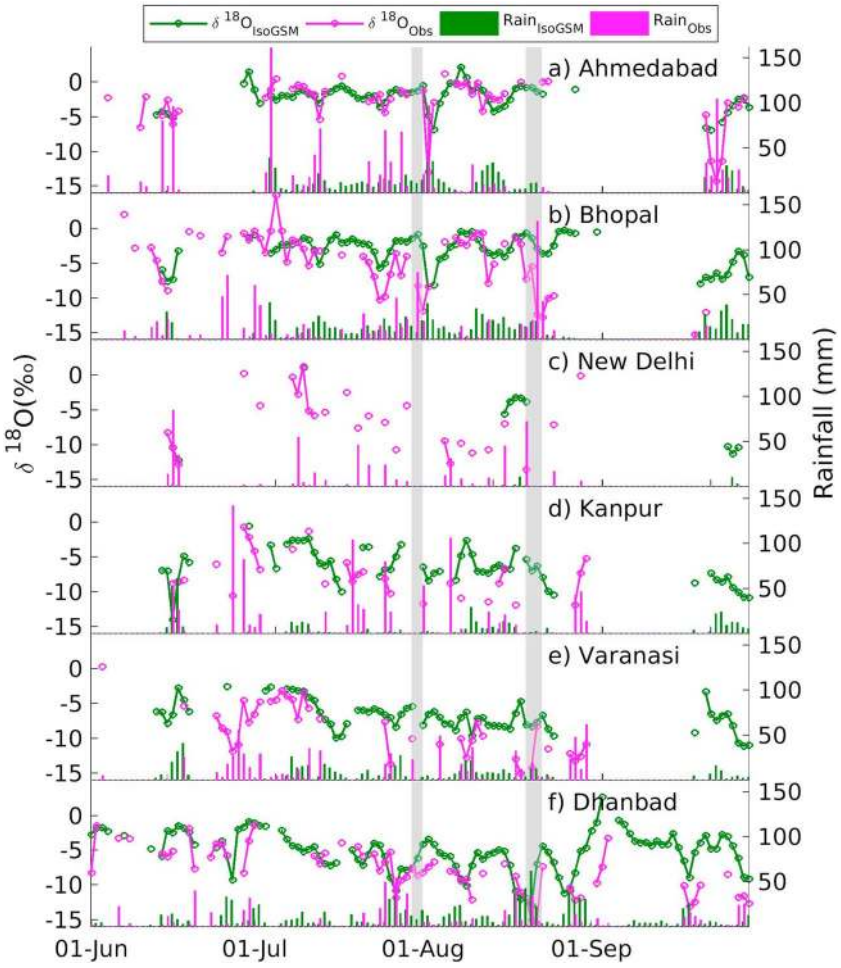

Figure 3. Time series of rainfall (vertical bars) and $\delta^{18}O_p$ (line and scatter) at each station (a–f); magenta lines/bars represent observations, and green lines/bars represent nudged IsoGSM simulations. Area highlighted using gray shades represent two monsoon depressions that occurred during the period of study. IsoGSM = Isotope-enabled Global Spectral Model.

As a result of nudging, the model simulated moisture flux is similar to the observations. Correlation coefficients between the simulated temporal variation of daily and GPCP rainfall are weak during monsoon 2013 (supporting information Figure SF1). These correlations are mostly insignificant over the northern Indian region. At all sampling stations, except Ahmedabad and Dhanbad, the simulated daily rainfall shows insignificant temporal correlation with the measured rain amount (Table 2). In contrast, the simulated temporal variability of $\delta^{18}O_p$ is significantly correlated with observed $\delta^{18}O_p$ (Table 2), except at New Delhi, where the model has a significant dry bias (Figure 3c). That is, the model-predicted intraseasonal variation of $\delta^{18}O_p$ is closer to the observations than the model rainfall. This may be due to the dominant control of moisture transport pathways on $\delta^{18}O_p$ variability and is discussed in the next section.

3.4. Role of Circulation (Moisture Transport Pathways) on $\delta^{18}O_p$ Variability

3.4.1. Back Trajectory Analyses

Composites of trajectory densities for ^{18}O-enriched, median and ^{18}O-depleted events were calculated and depicted in Figure 5, and the difference between ^{18}O-enriched and ^{18}O-depleted events is shown in Figure 6. Rain during enriched events at Ahmedabad, Bhopal, and New Delhi is solely derived from the AS branch. Respectively 16.6%, 28.0%, and 14.6% of total rain at these stations occurred during ^{18}O-enriched events. At Ahmedabad and Bhopal, ^{18}O-depleted events (contributing 43.2% and 43.8% of total rain, respectively) are associated with the trajectories both from the AS and BoB branches, but the BoB branch slightly dominates. About 49.2% of the total rain at New Delhi occurred during ^{18}O-depleted events with a relatively higher number of trajectories of the BoB branch. Median ^{18}O events at Ahmedabad (40.2% of the total rain)

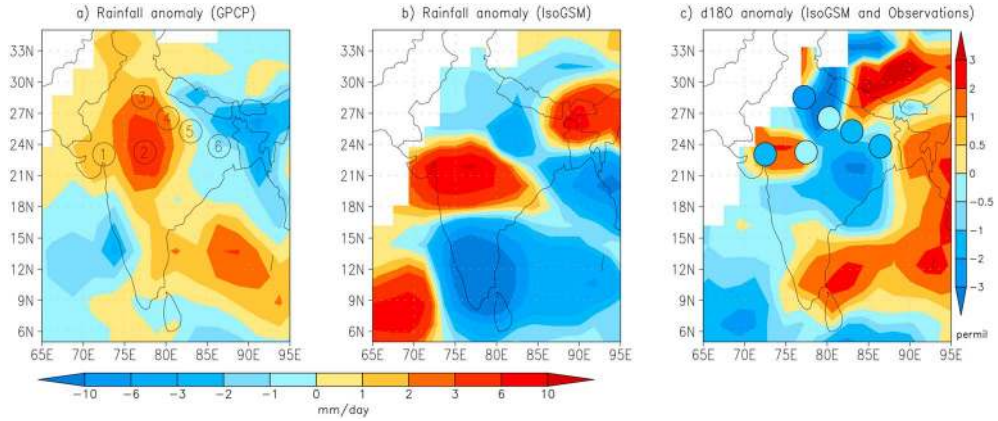

Figure 4. (a) Observed (GPCP) and (b) simulated (IsoGSM) rainfall anomalies (mm/day) during ISM 2013. Climatology is calculated for the period 1980–2007. (c) $\delta^{18}O_p$ anomalies (‰) during ISM 2013; shaded contours are the IsoGSM simulations, and circles are observations. For calculating observed $\delta^{18}O_p$ anomalies, climatological ISM $\delta^{18}O_p$ were constructed using IsoMAP. Sample collection stations used in this study are highlighted in (a) (refer to Figure 1 for station names). GPCP = Global Precipitation Climatology Project; IsoGSM = Isotope-enabled Global Spectral Model.

and Bhopal (28.2% of the total rain) are mainly characterized by moisture transport through the AS branch with a little contribution from the BoB branch. Median events at New Delhi (36.2% of the total rain) are solely contributed by the AS branch, but the trajectories are clustered to form a narrow path, slightly southward of the trajectories associated with ^{18}O enriched events. Generally, at these three stations, anomalous trajectory densities over the AS branch are observed during ^{18}O-enriched events, whereas the most ^{18}O-depleted events are characterized by more trajectories through the BoB branch (Figures 5 and 6).

At Kanpur, Varanasi, and Dhanbad 13.8%, 20.9%, and 20.2% of the total rain, respectively, occurred during the ^{18}O-enriched events. During these events at Dhanbad, trajectories originate from the Arabian Sea and mostly advance to the station via the head Bay of Bengal, while the trajectories reaching Kanpur and Varanasi very rarely pass through the BoB (Figure 5). During median (55.9%, 26.2%, and 41.5% of the total rain at Kanpur, Varanasi, and Dhanbad) and ^{18}O-depleted events at these stations (30.3%, 52.9%, and 38.3% of the total rain, respectively), both branches are present in the trajectories. Also, at Kanpur, more AS branch (BoB branch) trajectories are observed during ^{18}O-enriched (depleted) events (Figure 6). At Varanasi, trajectories during depleted events pass through the northern Indian region while the enriched events are characterized by more trajectories passing through the central Indian region. At Dhanbad, southwesterly trajectories through the AS branch slightly dominate during ^{18}O-enriched events.

Observed differences in trajectory densities during ^{18}O-depleted and ^{18}O-enriched events are compared with the IsoGSM results (Figure 6). IsoGSM also produces ^{18}O-depleted (enriched) rain events associated with the anomalous air parcel trajectories through the BoB branch (AS branch) at four out of six stations. At Varanasi and Dhanbad, simulated trajectory-$\delta^{18}O_p$ relations are not consistent with the observations.

Switching between the BoB and the AS branch has little influence on $\delta^{18}O_p$ variability at Dhanbad and Varanasi. The main reason for this could be as follows: when the AS branch provides moisture to the other four stations, it takes a shorter path from the moisture source (the ocean) and encounters relatively low rainfall/convection enroute compared to those of the BoB branch. These conditions do not hold for the stations Dhanbad and Varanasi (Figure 5). JJAS mean outgoing longwave radiation (OLR) during 2013 (supporting information Figure SF5) also suggests that both the AS and BoB branches pass through the convectively active region (OLR $<$ 210 W/m^2) before they reach these stations and thus may result in diminishing the isotopic distinction between the two branches.

3.4.2. Role of Rainfall Along the Back Trajectories

Over the tropical oceans, a negative correlation between $\delta^{18}O$ of boundary layer vapor and upstream rainfall has been previously reported (Kurita, 2013; Midhun et al., 2013) and the same fact is used here to check the role of $\delta^{18}O$ of the advected vapor on $\delta^{18}O_p$ variability. Such a relation would be a cumulative effect of advection on the remnant vapor after the rainout (Rayleigh distillation model, Gat & Gonfiantini, 1981) as well as the

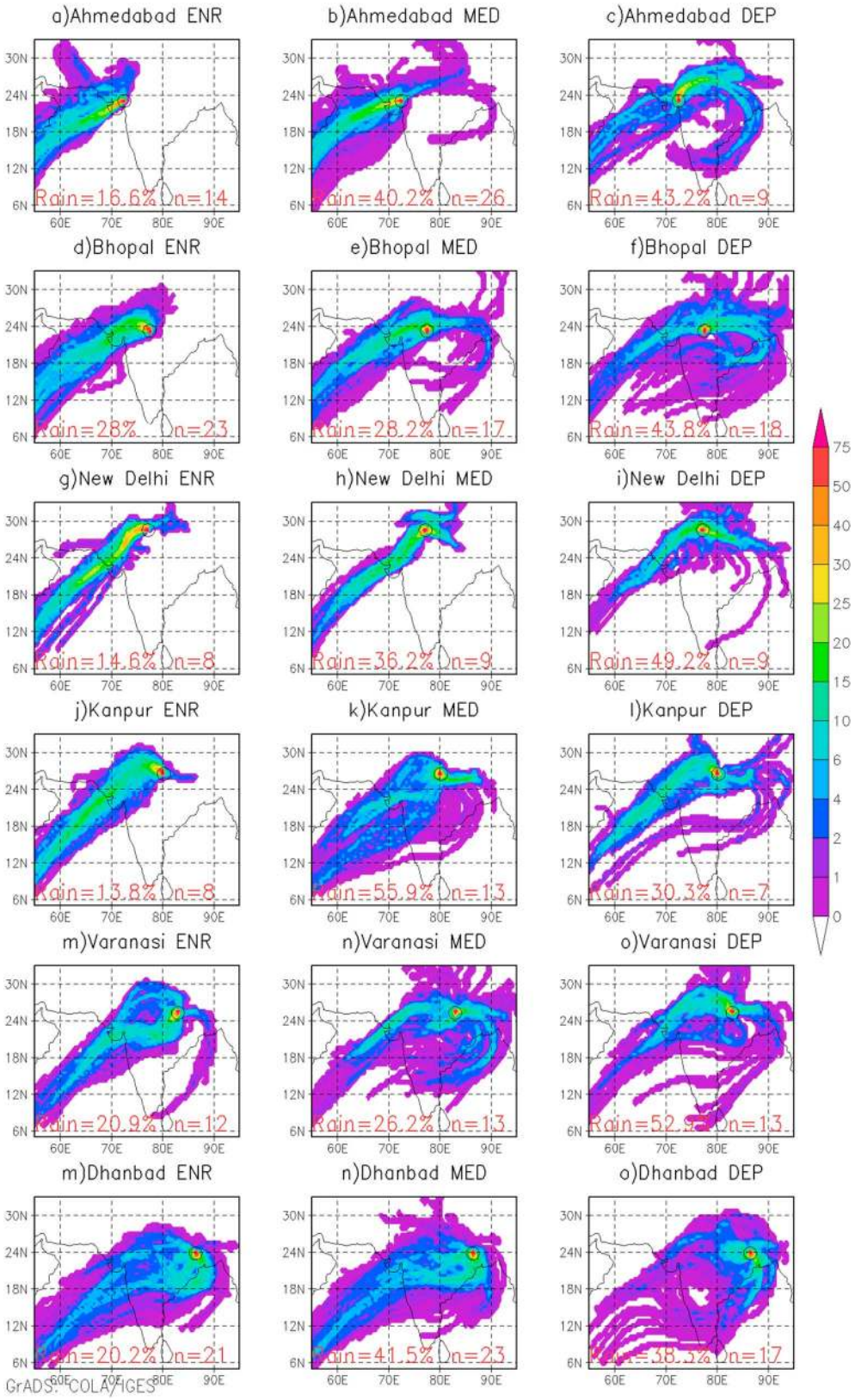

Figure 5. (a–o) Trajectory density (in %) during ^{18}O-enriched (ENR), ^{18}O median (MED), and ^{18}O-depleted events (DEP). Please refer to the text for event classification. Number of events (*n*) and percentage of rainfall (rain %) contributed by each group are also shown.

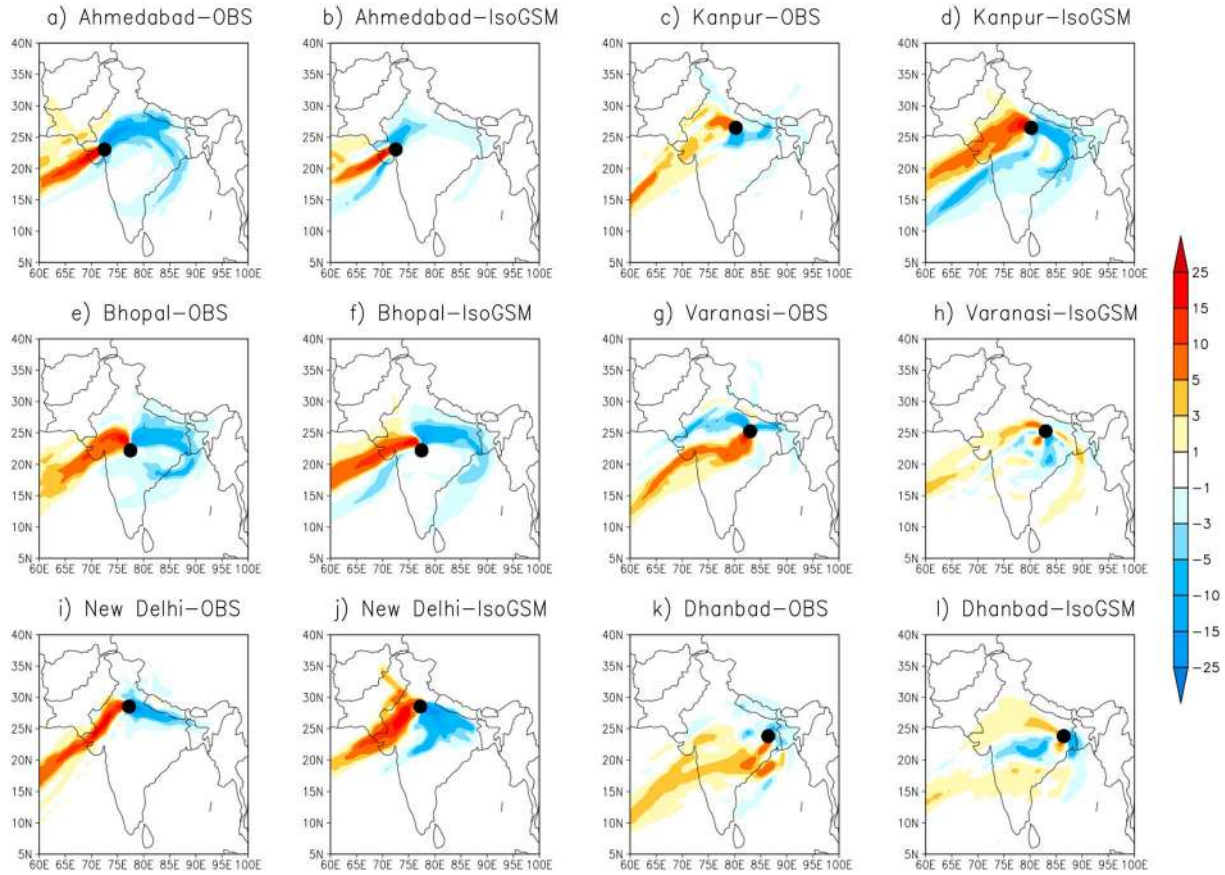

Figure 6. (a–l) Difference in the trajectory density (in %) between ^{18}O-enriched and ^{18}O-depleted events. Positive (negative) values represent higher trajectory density during enriched (depleted) events.

rain-vapor interactions in the convective systems along the trajectory. At stations except Varanasi and Kanpur, $\delta^{18}O_p$ is well correlated with total rainfall along the back trajectory (i.e., upstream rainfall; Figure 7a). These relations become stronger with increasing back trajectory hours and stabilize after ~5 days. This suggests that daily $\delta^{18}O_p$ likely reflects a 5-day integrated convective activity along the moisture transport pathways. These results are consistent with IsoGSM simulations too (Figure 7b). A similar role of upwind convection on isotopic variability over tropical Andes (Samuels-Crow et al., 2014) and Central Andes has been previously reported (Fiorella et al., 2015). Thus, the strong influence of upstream rainfall can be a possible reason for the lack or weak local amount effect over the region (Lee et al., 2012; Midhun & Ramesh, 2016).

To understand the processes of those related rainfall along the trajectory with $\delta^{18}O_p$ inside the model (IsoGSM), we plotted the relationship between column-integrated water content (precipitable water) and its isotopic composition along the 10-day back trajectories. Three most ^{18}O-enriched events and three most ^{18}O-depleted events at each station are selected for this analysis (Figure 8). A general negative relationship between precipitable water and its $\delta^{18}O$ is observed during ^{18}O-depleted events at all stations except New Delhi. This relationship is opposite to the Rayleigh distillation prediction, according to which the rainout along the trajectories decreases precipitable water and $\delta^{18}O$ of the remnant vapor. A positive relation between precipitable water $\delta^{18}O$ and OLR is also observed along the trajectory during ^{18}O-depleted events. This means that strong upstream convection reduces the ^{18}O content of the precipitable water, and the strong recycling and moisture convergence (Moore et al., 2014; Risi et al., 2008; Wei et al., 2018) in such systems increases the precipitable water content along the trajectory. This creates the counterintuitive negative relationship between precipitable water and its $\delta^{18}O$ along the trajectory during depleted events (Wei et al., 2018). This mechanism breaks down during ^{18}O-enriched events, implying that intensity of convection plays a significant role in determining the $\delta^{18}O$ of advected vapor.

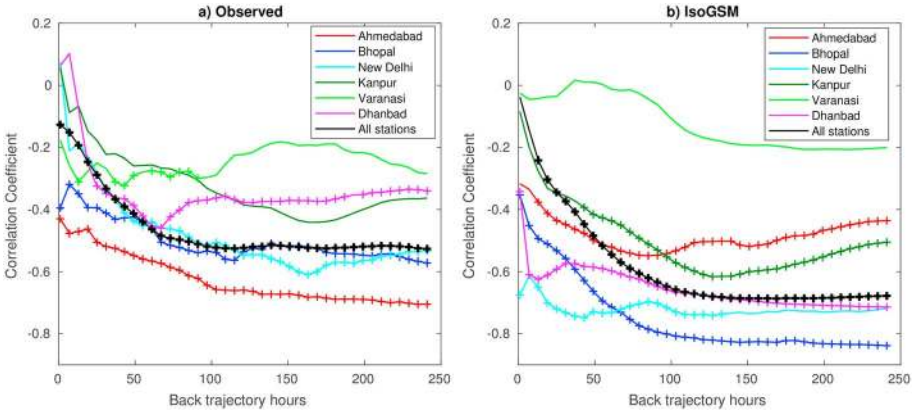

Figure 7. (a) Relation between $\delta^{18}O_p$ and the average rain (TRMM) along the back trajectory with varying back trajectory hours. The "+" symbol represents correlations that are significant at $P < 0.05$ level. (b) Same as (a) but for IsoGSM simulations. TRMM = Tropical Rainfall Measuring Mission; IsoGSM = Isotope-enabled Global Spectral Model.

3.4.3. Moisture Flux Analysis

Correlation analysis between $\delta^{18}O_p$ and the meridional component of vertically integrated moisture flux (Q_v) helps to understand the role of moisture transport pathways on $\delta^{18}O_p$. When the AS branch dominates, Q_v would be positive over the areas west to the stations and $\delta^{18}O_p$ is expected to be higher. Similarly, when the BoB branch dominates, Q_v would be positive over areas east of the stations and $\delta^{18}O_p$ would be more negative. Hence, we anticipate a dipole pattern in the Q_v-$\delta^{18}O_p$ correlations with positive correlations

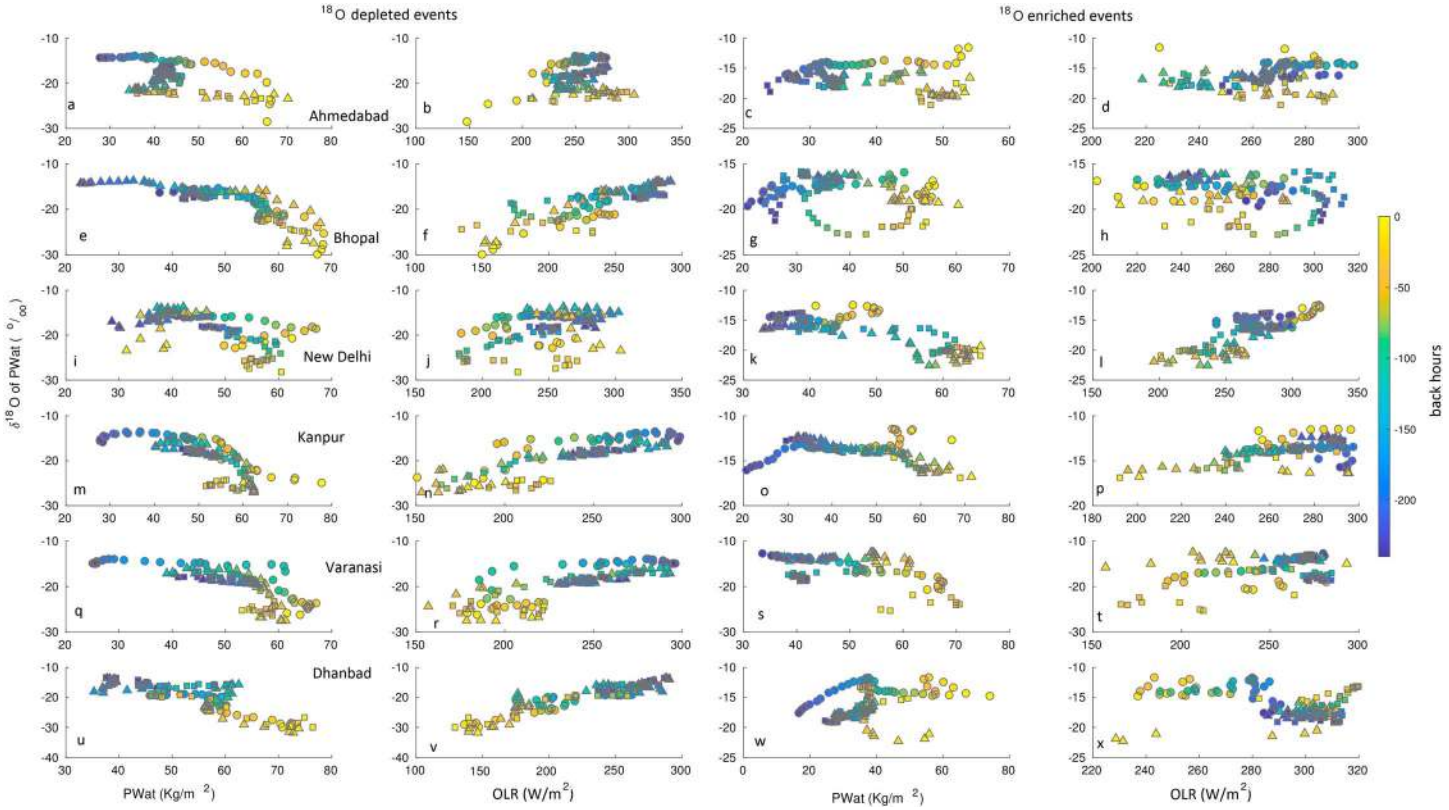

Figure 8. Relationship of precipitable water $\delta^{18}O$ with precipitable water content (PWat, first and third columns) and OLR (second and fourth columns) along the trajectory for three most ^{18}O-depleted events and ^{18}O-enriched events at each sampling station as simulated by IsoGSM. Three symbols (circle, triangle, and square) represent three different events, and the color indicates back trajectory hours. Each panel corresponds to each station. OLR = outgoing longwave radiation; IsoGSM = isotope-enabled GCM.

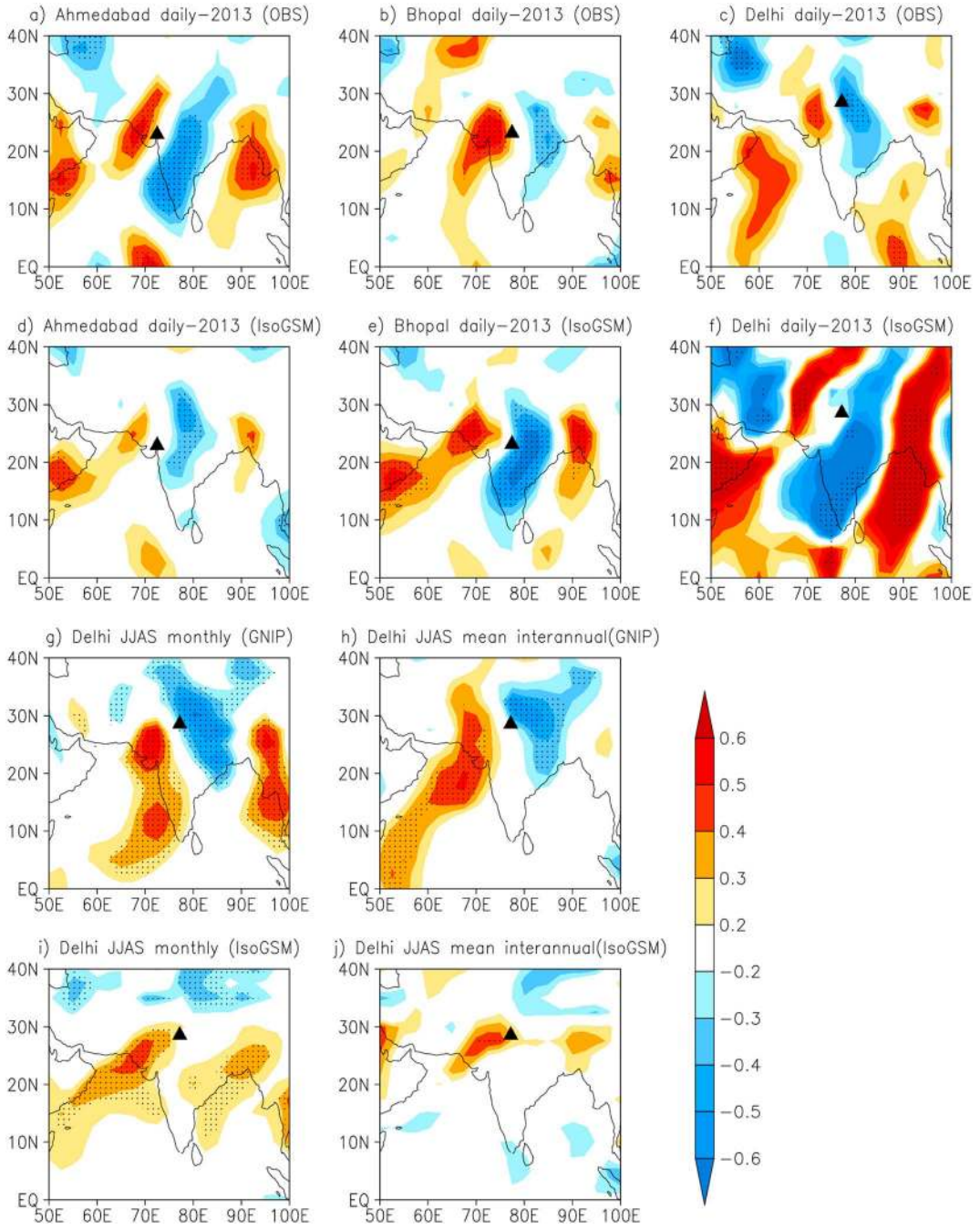

Figure 9. Correlation between $\delta^{18}O_p$ and meridional moisture transport vectors (Q_v). (a–c) Correlations between observed $\delta^{18}O_p$ and Q_v (NCEP) at stations Ahmedabad, Bhopal, and New Delhi during ISM 2013. (d–f) Same as (a–c) but for the IsoGSM simulations. (g and h) Observed $\delta^{18}O_p$-Q_v correlations on monthly and interannual timescales during ISM at New Delhi. (i and j) Same as (g and h) but for IsoGSM simulations. Black dots represent significant correlations at $P < 0.05$ level. The filled triangle represents the location of sampling stations. NCEP = National Center for Environmental Prediction; ISM = Indian Summer Monsoon; IsoGSM = Isotope-enabled Global Spectral Model.

over the area west to the stations and negative correlation over the areas east to the station. This pattern is observed in our correlation analysis for Ahmedabad, Bhopal, and New Delhi (Figure 9). When it comes to IsoGSM simulations, this relationship between $\delta^{18}O_p$ and Q_v is well captured for Ahmedabad and Bhopal (Figure 9) but not over New Delhi. Again, the model's failure is likely due to the dry bias in the modeled ISM rainfall over New Delhi (only 11 of the 26 rainy days are simulated during ISM 2013 at New Delhi, Figure 3c).

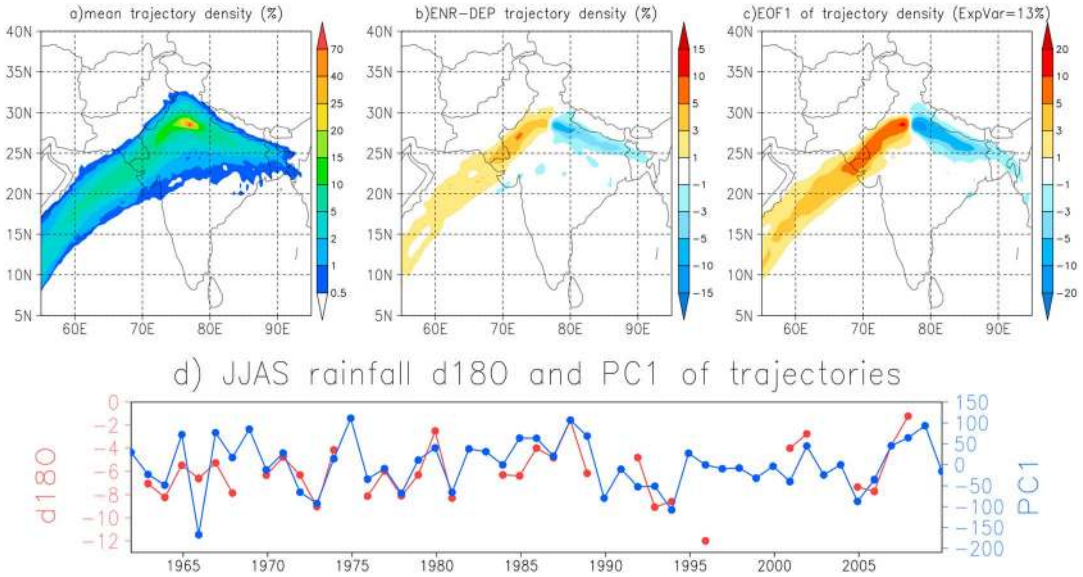

Figure 10. (a) Mean JJAS trajectory density (in percent) for GNIP station New Delhi. (b) Difference in ISM trajectory densities between composites of enriched and depleted years. (c) Empirical Orthogonal Function (EOF1) of JJAS mean of ISM trajectories. (d) Time series of JJAS mean $\delta^{18}O_p$ (red) and PC1 (blue) of JJAS mean ISM trajectories at New Delhi. Correlation (r) between mean $\delta^{18}O_p$ and PC1 is 0.58 ($P < 0.05$). JJAS = June–September; ISM = Indian Summer Monsoon.

Validity of $\delta^{18}O_p$ and Q_v relation over New Delhi on monthly (individual months of JJAS) and interannual timescales (JJAS means) is also verified using long-term GNIP data set and found to be significant (Figures 9g and 9h). Again, it should be noted that IsoGSM fails to capture this relation over New Delhi on monthly and interannual timescales (Figures 9i and 9j).

3.4.4. Interannual Variability of $\delta^{18}O_p$ at New Delhi

The effect of moisture transport pathways on $\delta^{18}O_p$ is clearly demonstrated in the previous sections (3.4.1 and 3.4.2). Additionally, a $\delta^{18}O_p$-Q_v relationship is also observed over New Delhi on the interannual timescale (Figures 9g and 9h). To quantify the role of changing moisture transport pathway on interannual variability of ISM $\delta^{18}O_p$ at New Delhi, we extended the back trajectory analysis to the period 1961 to 2009. The climatological mean trajectory density is depicted in Figure 9a. Differences between the composite trajectory densities for years with ^{18}O-depleted and ^{18}O-enriched rain are shown in Figure 9b. This pattern is very similar to the one observed during 2013 (Figure 6i) on an intraseasonal timescale, suggesting the strong influence of circulation also on interannual variations of ISM $\delta^{18}O_p$ over New Delhi. To check the leading mode of variability of back trajectory, we performed empirical orthogonal function analysis on trajectory density anomalies. Interestingly, the leading mode (first Empirical Orthogonal Function, EOF-1, explained variance is ~13%, Figure 10c) is very similar to the trajectory density anomaly pattern shown in Figure 9b. Approximately 34% of the interannual variability of ISM $\delta^{18}O_p$ at New Delhi is explained by the first Principal Component (PC1) of trajectory densities (Figure 10d), whereas the local amount effect explains only ~16%. This analysis suggests that the dual moisture source has a more significant role in modulating monsoon $\delta^{18}O_p$ on daily to interannual timescales over this region. Sinha et al. (2015) suggested that the enhanced moisture transport from the BoB branch co-occurs with wet months/years of monsoon and thus creates an amount effect at New Delhi. However, in our analysis JJAS mean rainfall does not correlate with PC1 of trajectory densities suggesting that local rainfall amount and variations in moisture transport pathways independently drive the $\delta^{18}O_p$ variability at New Delhi. A multilinear regression of $\delta^{18}O_p$ with PC1 and rainfall is able to explain 47% of the $\delta^{18}O_p$ variability at New Delhi on the interannual timescale (Table 3).

3.5. Spatial Pattern of $\delta^{18}O_p$ and the Continental Effect

Previously reported ISM $\delta^{18}O_p$ values, archived at GNIP, are interpolated using IsoMAP (Figure 11c). The spatial distribution of ISM $\delta^{18}O_p$ during 2013 is in good agreement with the climatological IsoMAP estimates. Figure 11d depicts an independent estimate of climatological ISM $\delta^{18}O_p$ from three IsoGSMs that are

Table 3
Linear and Multilinear Regression of JJAS Mean $\delta^{18}O_p$ With PC1 of JJAS Mean Trajectory Densities and JJAS Mean Rainfall at GNIP Station New Delhi

Regression	r^2
$\delta^{18}O_p = (-5.93 \pm 0.34) + (0.021 \pm 0.005) \times PC1$	0.34
$\delta^{18}O_p = (-3 \pm 1) + (-0.004 \pm 0.001) \times rainfall$	0.16
$\delta^{18}O_p = (-3 \pm 1) + (-0.004 \pm 0.001) \times rainfall + (0.021 \pm 0.004) \times PC1$	0.47

Note. JJAS = June–September.

nudged with reanalysis wind fields (SWING2 models, Midhun & Ramesh, 2016). Both the observations and SWING2 simulations show a strong influence of large-scale low-level winds (Figure 11a) on the spatial pattern of ISM $\delta^{18}O_p$: the progressive depletion of $\delta^{18}O_p$ along the low-level south westerlies (also called low-level jet) from the Arabian Sea region to northeastern parts of India can be qualitatively explained using the classical Rayleigh model. Interestingly, no isotope minima corresponding to the rainfall maxima (Western Ghats and Myanmar coast, Figure 11b) are observed in the ISM region, implying a weak or insignificant role of the local amount effect on the spatial distribution of ISM $\delta^{18}O_p$.

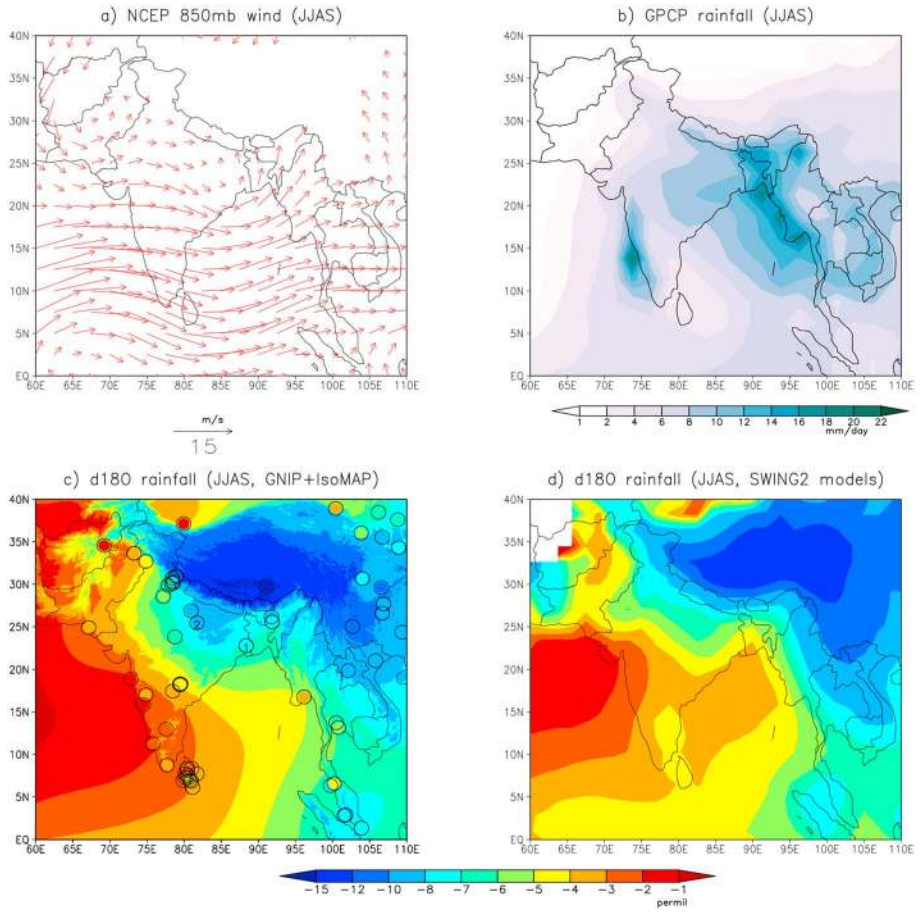

Figure 11. (a) Climatological JJAS mean wind at the 850-hPa level (NCEP, unit: meter per second). (b) Climatological mean ISM rainfall (GPCP, unit: millimeter per day). (c) Observed climatological mean ISM $\delta^{18}O_p$ (filled circles) and as predicted by IsoMAP (shaded). (d) GCM simulated (multimodel mean from SWING2 models, Midhun & Ramesh, 2016) climatological mean ISM $\delta^{18}O_p$. Locations of Kolkata (1) and Allahabad (2) are indicated by numbers in (c). JJAS = June–September; NCEP = National Center for Environmental Prediction; ISM = Indian Summer Monsoon; GPCP = Global Precipitation Climatology Project; GCM = General Circulation Model.

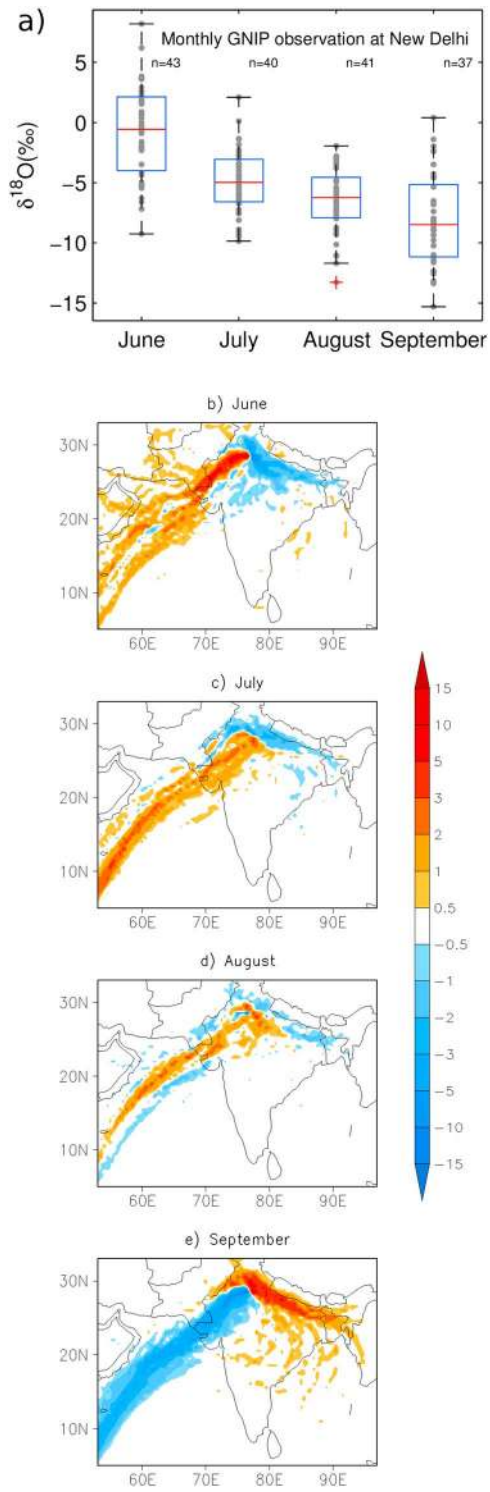

Figure 12. (a) Box and whisker plot showing the distribution of monthly $\delta^{18}O_p$ observations at GNIP station New Delhi. Gray circles show the individual observations. (b–e) Climatological average deviations in trajectory densities from JJAS mean trajectories during June, July, August, and September.

Previous studies hypothesized a possibility of the continental effect along the Indo-Gangetic plain (from the head bay of Bengal to New Delhi) as a result of the propagation of monsoon storms formed over the BoB (Krishnamurthy & Bhattacharya, 1991; Sengupta & Sarkar, 2006). Krishnamurthy and Bhattacharya (1991) suggested a continental effect (depletion by ~2‰ for 1,300 km) in the ISM rainfall over this plain by analyzing $\delta^{18}O$ of ground waters. But this is neither observed in GNIP $\delta^{18}O_p$ (Figure 11c) nor in our observations along this sector. GNIP observations show depletion in $\delta^{18}O_p$ at Allahabad (a GNIP station, ~120 km from Varanasi) by 2‰ compared to that at Kolkata (a coastal station near the head bay of Bengal). A similar $\delta^{18}O_p$ depletion of 0.8‰ is observed at Varanasi compared to Dhanbad in our observations. But no further $\delta^{18}O_p$ depletion toward New Delhi is observed both in GNIP and in our observations. Sengupta and Sarkar (2006) suggested that the $\delta^{18}O_p$ enrichment along the Allahabad-Delhi sector is possibly due to the contributions from the $\delta^{18}O$-enriched vapor by evapotranspiration as well as from the AS branch of moisture transport. Our study confirms the role of the AS branch of moisture transport at New Delhi and Kanpur modulating the spatial distribution of $\delta^{18}O_p$ along the Indo-Gangetic plain.

3.6. Depleting Trend in $\delta^{18}O_p$ During the ISM Season

All except Ahmedabad and New Delhi show a significant temporal decreasing trend in $\delta^{18}O_p$ during the ISM season (supporting information Figure SF2). This trend is not statistically significant at New Delhi due to a continuous 3-day ^{18}O-depleted rainfall event during the initial period of ISM season 2013. Long-term observations at New Delhi, however, do show a statistically significant trend in $\delta^{18}O_p$ during the ISM season (Figure 12). Similar depletion trends of $\delta^{18}O_p$, as the ISM season advances, were reported earlier as well (Breitenbach et al., 2010; Sengupta & Sarkar, 2006; Srivastava et al., 2014). Sengupta and Sarkar (2006) proposed that a similar trend in Kolkata could be due to the shift in the origin of the monsoon depression from northern to southern (below 15°N) BoB, resulting in a longer condensation history of the air parcel and more ^{18}O-depleted rain over Kolkata. Later Breitenbach et al. (2010) attributed this depletion to the formation of a freshwater plume in the head Bay of Bengal by ^{18}O-depleted discharge from the Ganga-Brahmaputra river system. The estimated reduction in $\delta^{18}O$ of surface water at the head Bay of Bengal can be up to −4.5‰; however, the average of observed $\delta^{18}O$ of surface water over the BoB during the end of the season is ~ −0.4‰ (Achyuthan et al., 2013; Sengupta et al., 2013; Singh et al., 2010). We also estimated the possible value of $\delta^{18}O$ of surface water at the head Bay of Bengal from climatological salinity (S) data using the reported $\delta^{18}O$-S relations (Sengupta et al., 2013; Singh et al., 2014) and the estimated $\delta^{18}O$ of surface water varied from −0.2‰ to −0.8‰ (for September). Thus, the evaporation from this freshwater plume cannot contribute to the observed trend in $\delta^{18}O_p$ (Lekshmy et al., 2015). We observe that over the inland station New Delhi, this trend (Figure 11) co-occurs with the switching of moisture transport pathway from the AS branch to the BoB branch as the ISM season advances. But the cause for similar trends observed over the stations closer to the head Bay of Bengal is not clear yet.

4. Conclusions

A new data set of ISM $\delta^{18}O_p$ and δD_p from six stations across northern and central India during the year 2013 is presented. The local and remote factors that control ISM $\delta^{18}O_p$ are further investigated along with the nudged simulations from an IsoGSM and previously reported observations.

ISM $\delta^{18}O_p$ at all the stations for 2013 is found to be relatively lower compared to their climatological means in the observations (GNIP and IsoMAP). A local amount effect is observed on daily timescales in the ISM rainfall at five out of six stations during 2013, but it explains only 7% to 23% of total $\delta^{18}O_p$ variance. The observed strong correlation between average rainfall along the air parcel back trajectory and $\delta^{18}O_p$ highlights the role of upstream convective activities on ISM $\delta^{18}O_p$. Further analysis using HYSPLIT and moisture flux calculations revealed the role of moisture transport pathways on $\delta^{18}O_p$ variability at Ahmedabad, Bhopal, and New Delhi: anomalous moisture transport along the AS branch (BoB branch) results in relatively ^{18}O-enriched (depleted) rainfall at these stations. We also found that the same mechanism operates on an interannual timescale at New Delhi, and it explains a significant portion (~34%) of interannual variability of ISM $\delta^{18}O_p$.

Similar to the observations, IsoGSM-simulated ISM $\delta^{18}O_p$ at most of the stations are also lower compared to its climatology. IsoGSM captures the overall spatial distribution of ISM rainfall during 2013, but it fails to capture the northwestern limit of rainfall as well as the intraseasonal variability of rainfall over the sampling stations. However, the simulated temporal variability of ISM $\delta^{18}O_p$ is consistent with observations, possibly due to the control of large-scale circulation on simulated $\delta^{18}O_p$ values. Back trajectory analysis using IsoGSM also highlights the importance of variability of moisture transport pathways on ISM $\delta^{18}O_p$.

Finally, we hypothesize that the effect of circulation on ISM $\delta^{18}O_p$ variability is due to (1) switching of moisture transport pathways between the AS and BoB branches and (2) the variability in convective history along both moisture transport pathways. The atmosphere above the BoB is more convectively active compared to the AS during ISM (Krishnamurthy & Ajayamohan, 2010). It is well known that organized convection leads to a higher depletion in ^{18}O of both the rainfall and boundary layer vapor (Kurita, 2013; Lekshmy et al., 2014). Therefore, an air parcel that travels through the BoB and surrounding convectively active region is more likely to have relatively depleted ^{18}O values which will be reflected in the subsequent precipitation. It should also be noted that the BoB branch of trajectories takes a longer path over the rainfall region of ISM (Figures 2 and 4) which in turn causes a higher depletion in ^{18}O. Apart from these, the AS branch can also cause relatively more negative $\delta^{18}O_p$ if it encounters anomalously high convective activity along its path during that particular rainfall spell, especially over the areas around Dhanbad and Varanasi. Our overall analyses suggest strong influence of upstream process on $\delta^{18}O_p$ variability in the study area, which is responsible for the weak amount effect.

Over central and northern India, the BoB branch of moisture transport is often associated with inland movement of the monsoon depression from the BoB, one of the key indicators of ISM intensity, which will be recorded in $\delta^{18}O_p$. Proxies from areas adjoining Ahmedabad, Bhopal, and Varanasi would primarily reflect the intrusion of these westward/northwestward moving monsoon depressions in their $\delta^{18}O$ or δD. A recent study (Sarkar et al., 2015), using multiproxy records in Lonar lake from central India, interpreted low leaf wax δD values as a switching of the AS branch to the BoB branch during the mid-Holocene. Such interpretations not only reconstruct the past hydroclimate but also help constrain paleo-atmospheric circulation simulated by climate models.

Acknowledgments
We thank Valérie Masson-Delmotte for the discussions during the initial stages of the work. We thank ISRO-GBP for funding. We thank Ramya Sunder Raman, Kripa Shankar, Hari, Saurabh Singh, and Masood for their help during the sample collection. Daily rainfall and isotope data generated by this study are given as a supporting information. GNIP data used in this study can be accessed from https://nucleus.iaea.org/wiser/gnip.php. TRMM, GPCP, and NCEP data were obtained from https://pmm.nasa.gov/data-access/downloads/trmm, https://precip.gsfc.nasa.gov/gpcp_daily_comb.html, and https://www.esrl.noaa.gov/psd/data/gridded/data.ncep.reanalysis.html, respectively. IsoGSM simulation used in this study is available at http://hydro.iis.u-tokyo.ac.jp/~kei/tmp/isogsm2.

References

Achyuthan, H., Deshpande, R. D., Rao, M. S., Kumar, B., Nallathambi, T., Shashi Kumar, K., et al. (2013). Stable isotopes and salinity in the surface waters of the bay of Bengal: Implications for water dynamics and palaeoclimate. *Marine Chemistry*, *149*, 51–62. https://doi.org/10.1016/j.marchem.2012.12.006

Adler, R. F., Huffman, G. J., Chang, A., Ferraro, R., Xie, P.-P., Janowiak, J., et al. (2003). The version-2 global precipitation climatology project (GPCP) monthly precipitation analysis (1979–present). *Journal of Hydrometeorology*, *4*(6), 1147–1167. https://doi.org/10.1175/1525-7541(2003)004%3C1147:TVGPCP%3E2.0.CO;2

Ahmad, M., Aggarwal, P., van Duren, M., Poltenstein, L., Araguas, L., Kurttas, T., & Wassenaar, L. I. (2012). Final report on fourth interlaboratory comparison exercise for $\delta 2H$ and $\delta^{18}O$ analysis of water samples (WICO2011).

Berkelhammer, M., Sinha, A., Mudelsee, M., Cheng, H., Yoshimura, K., & Biswas, J. (2013). On the low frequency component of the ENSO-Indian monsoon relationship: A paired proxy perspective. *Climate of the Past Discussions*, *9*(3), 3103–3123. https://doi.org/10.5194/cpd-9-3103-2013

Bowen, G. J. (2010). Statistical and geostatistical mapping of precipitation water isotope ratios. In *Isoscapes* (pp. 139–160). Dordrecht, Netherlands: Springer. https://doi.org/10.1007/978-90-481-3354-3_7

Breitenbach, S. F. M., Adkins, J. F., Meyer, H., Marwan, N., Kumar, K. K., & Haug, G. H. (2010). Strong influence of water vapor source dynamics on stable isotopes in precipitation observed in southern Meghalaya, NE India. *Earth and Planetary Science Letters*, *292*(1–2), 212–220. https://doi.org/10.1016/j.epsl.2010.01.038

Dansgaard, W. (1964). Stable isotopes in precipitation. *Tellus*, *16*(4), 436–468. https://doi.org/10.1111/j.2153-3490.1964.tb00181.x

Deshpande, R. D., Maurya, A. S., Kumar, B., Sarkar, A., & Gupta, S. K. (2010). Rain-vapor interaction and vapor source identification using stable isotopes from semiarid western India. *Journal of Geophysical Research*, *115*, D23311. https://doi.org/10.1029/2010JD014458

Draxler, R. R., & Rolph, G. D. (2003). HYSPLIT (HYbrid single-particle Lagrangian integrated trajectory) model access via NOAA ARL READY website (http://www.arl.noaa.gov/ready/hysplit4.html). NOAA Air Resources Laboratory, Silver Spring, MD.

Ebisuzaki, W. (1997). A method to estimate the statistical significance of a correlation when the data are serially correlated. *Journal of Climate*, *10*(9), 2147–2153. https://doi.org/10.1175/1520-0442(1997)010%3C2147:AMTETS%3E2.0.CO;2

Epstein, S., & Mayeda, T. (1953). Variation of O 18 content of waters from natural sources. *Geochimica et Cosmochimica Acta*, *4*(5), 213–224. Retrieved from http://www.sciencedirect.com/science/article/pii/0016703753900519. https://doi.org/10.1016/0016-7037(53)90051-9

Fiorella, R. P., Poulsen, C. J., Pillco Zolá, R. S., Barnes, J. B., Tabor, C. R., & Ehlers, T. A. (2015). Spatiotemporal variability of modern precipitation $\delta^{18}O$ in the Central Andes and implications for paleoclimate and paleoaltimetry estimates. *Journal of Geophysical Research: Atmospheres*, *120*, 4630–4656. https://doi.org/10.1002/2014JD022893

Gadgil, S., & Gadgil, S. (2006). The Indian monsoon. *GDP and agriculture. Economic and Political Weekly*, 4887–4895.

Gat, J. R., & Gonfiantini, R. (1981). Stable isotope hydrology. Deuterium and oxygen-18 in the water cycle. Technical Reports Series 210. Vienna: IAEA Technical Reports Series 210. Retrieved from https://inis.iaea.org/search/search.aspx?orig_q=RN:13677657

Goddard Earth Sciences Data and Information Services Center (2016). TRMM (TMPA) precipitation L3 1 day 0.25 degree x 0.25 degree V7. Retrieved June 1, 2016, from https://disc.gsfc.nasa.gov/datacollection/TRMM_3B42_Daily_7.html

Harris, I., Jones, P. D., Osborn, T. J., & Lister, D. H. (2014). Updated high-resolution grids of monthly climatic observations—The CRU TS3. 10 dataset. *International Journal of Climatology*, *34*(3), 623–642. https://doi.org/10.1002/joc.3711

Horita, J. (1988). Hydrogen isotope analysis of natural waters using an H2-water equilibration method: A special implication to brines. *Chemical Geology: Isotope Geoscience Section*, *72*(1), 89–94. https://doi.org/10.1016/0168-9622(88)90040-1

Kalnay, E., Kanamitsu, M., Kistler, R., Collins, W., Deaven, D., Gandin, L., et al. (1996). The NCEP/NCAR 40-year reanalysis project. *Bulletin of the American Meteorological Society*, *77*(3), 437–471. https://doi.org/10.1175/1520-0477(1996)077%3C0437:TNYRP%3E2.0.CO;2

Kanamitsu, M., Ebisuzaki, W., Woollen, J., Yang, S.-K., Hnilo, J. J., Fiorino, M., & Potter, G. L. (2002). NCEP-Doe AMIP-II reanalysis (R-2). *Bulletin of the American Meteorological Society*, *83*(11), 1631–1644. https://doi.org/10.1175/BAMS-83-11-1631

Krishnamurthy, R. V., & Bhattacharya, S. K. (1991). Stable oxygen and hydrogen isotope ratios in shallow ground waters from India and a study of the role of evapotranspiration in the Indian monsoon. *Stable Isotope Geochemistry: A Tribute to Samuel Epstein, Special Publication*, *3*, 187–203.

Krishnamurthy, V., & Ajayamohan, R. S. (2010). Composite structure of monsoon low pressure systems and its relation to Indian rainfall. *Journal of Climate*, *23*(16), 4285–4305. https://doi.org/10.1175/2010JCLI2953.1

Kumar, B., Rai, S. P., Kumar, U. S., Verma, S. K., Garg, P., Kumar, S. V. V., et al. (2010). Isotopic characteristics of Indian precipitation. *Water Resources Research*, *46*, W12548. https://doi.org/10.1029/2009WR008532

Kurita, N. (2013). Water isotopic variability in response to mesoscale convective system over the tropical ocean. *Journal of Geophysical Research: Atmospheres*, *118*, 10,376–10,390. https://doi.org/10.1002/jgrd.50754

Laskar, A. H., Ramesh, R., Burman, J., Midhun, M., Yadava, M. G., Jani, R. A., & Gandhi, N. (2015). Stable isotopic characterization of Nor'westers of southern Assam, NE India. *Journal of Climate Change*, *1*(1,2), 75–87. https://doi.org/10.3233/JCC-150006

Lee, J.-E., & Fung, I. (2008). "Amount effect" of water isotopes and quantitative analysis of post-condensation processes. *Hydrological Processes*, *22*(1), 1–8. https://doi.org/10.1002/hyp.6637

Lee, J.-E., Risi, C., Fung, I., Worden, J., Scheepmaker, R. A., Lintner, B., & Frankenberg, C. (2012). Asian monsoon hydrometeorology from TES and SCIAMACHY water vapor isotope measurements and LMDZ simulations: Implications for speleothem climate record interpretation. *Journal of Geophysical Research*, *117*, D15112. https://doi.org/10.1029/2011JD017133

Lekshmy, P. R., Midhun, M., & Ramesh, R. (2015). Spatial variation of amount effect over peninsular India and Sri Lanka: Role of seasonality. *Geophysical Research Letters*, *42*, 5500–5507. https://doi.org/10.1002/2015GL064517

Lekshmy, P. R., Midhun, M., Ramesh, R., & Jani, R. A. (2014). ^{18}O depletion in monsoon rain relates to large scale organized convection rather than the amount of rainfall. *Scientific Reports*, *4*, 5661. https://doi.org/10.1038/srep05661

Midhun, M., Lekshmy, P. R., & Ramesh, R. (2013). Hydrogen and oxygen isotopic compositions of water vapor over the bay of Bengal during monsoon. *Geophysical Research Letters*, *40*, 6324–6328. https://doi.org/10.1002/2013GL058181

Midhun, M., & Ramesh, R. (2016). Validation of $\delta^{18}O$ as a proxy for past monsoon rain by multi-GCM simulations. *Climate Dynamics*, *46*(5-6), 1371–1385. https://doi.org/10.1007/s00382-015-2652-8

Mitra, A. K., Momin, I. M., Rajagopal, E. N., Basu, S., Rajeevan, M. N., & Krishnamurti, T. N. (2013). Gridded daily Indian monsoon rainfall for 14 seasons: Merged TRMM and IMD gauge analyzed values. *Journal of Earth System Science*, *122*(5), 1173–1182. https://doi.org/10.1007/s12040-013-0338-3

Moore, M., Kuang, Z., & Blossey, P. N. (2014). A moisture budget perspective of the amount effect. *Geophysical Research Letters*, *41*, 1329–1335. https://doi.org/10.1002/2013GL058302

Pai, D. S., & Bhan, S. C. (2014). Monsoon 2013: A report (IMD met. Monograph no: ESSO/IMD/SYNOPTIC MET/01-2014/15). Retrieved from http://www.imd.gov.in/section/nhac/monsoon_report_2013.pdf

Risi, C., Bony, S., & Vimeux, F. (2008). Influence of convective processes on the isotopic composition ($\delta^{18}O$ and δD) of precipitation and water vapor in the tropics: 2. Physical interpretation of the amount effect. *Journal of Geophysical Research*, *113*, D19306. https://doi.org/10.1029/2008JD009943

Samuels-Crow, K. E., Galewsky, J., Hardy, D. R., Sharp, Z. D., Worden, J., & Braun, C. (2014). Upwind convective influences on the isotopic composition of atmospheric water vapor over the tropical Andes. *Journal of Geophysical Research: Atmospheres*, *119*, 7051–7063. https://doi.org/10.1002/2014JD021487

Sarkar, S., Prasad, S., Wilkes, H., Riedel, N., Stebich, M., Basavaiah, N., & Sachse, D. (2015). Monsoon source shifts during the drying mid-Holocene: Biomarker isotope based evidence from the core "monsoon zone" (CMZ) of India. *Quaternary Science Reviews*, *123*, 144–157. https://doi.org/10.1016/j.quascirev.2015.06.020

Sengupta, S., Parekh, A., Chakraborty, S., Ravi Kumar, K., & Bose, T. (2013). Vertical variation of oxygen isotope in bay of Bengal and its relationships with water masses. *Journal of Geophysical Research: Oceans*, *118*, 6411–6424. https://doi.org/10.1002/2013JC008973

Sengupta, S., & Sarkar, A. (2006). Stable isotope evidence of dual (Arabian Sea and bay of Bengal) vapour sources in monsoonal precipitation over North India. *Earth and Planetary Science Letters*, *250*(3–4), 511–521. https://doi.org/10.1016/j.epsl.2006.08.011

Sikka, D. R. (1977). Some aspects of the life history, structure and movement of monsoon depressions. *Pure and Applied Geophysics PAGEOPH*, *115*(5–6), 1501–1529. https://doi.org/10.1007/BF00874421

Singh, A., Jani, R. A., & Ramesh, R. (2010). Spatiotemporal variations of the δ^{18}O-salinity relation in the northern Indian Ocean. *Deep Sea Research Part I: Oceanographic Research Papers*, *57*(11), 1422–1431. https://doi.org/10.1016/j.dsr.2010.08.002

Singh, A., Mohiuddin, A., Ramesh, R., & Raghav, S. (2014). Estimating the loss of Himalayan glaciers under global warming using the δ^{18}O-salinity relation in the bay of Bengal. *Environmental Science & Technology Letters*, *1*(5), 249–253. https://doi.org/10.1021/ez500076z

Sinha, A., Kathayat, G., Cheng, H., Breitenbach, S. F. M., Berkelhammer, M., Mudelsee, M., et al. (2015). Trends and oscillations in the Indian summer monsoon rainfall over the last two millennia. *Nature Communications*, *6*. https://doi.org/10.1038/ncomms7309

Srivastava, R., Ramesh, R., & Rao, T. N. (2014). Stable isotopic differences between summer and winter monsoon rains over southern India. *Journal of Atmospheric Chemistry*, *71*(4), 321–331. https://doi.org/10.1007/s10874-015-9297-1

van Albada, S. J., & Robinson, P. A. (2007). Transformation of arbitrary distributions to the normal distribution with application to EEG test-retest reliability. *Journal of Neuroscience Methods*, *161*(2), 205–211. https://doi.org/10.1016/j.jneumeth.2006.11.004

Wei, Z., Lee, X., Liu, Z., Seeboonruang, U., Koike, M., & Yoshimura, K. (2018). Influences of large-scale convection and moisture source on monthly precipitation isotope ratios observed in Thailand, Southeast Asia. *Earth and Planetary Science Letters*, *488*, 181–192. https://doi.org/10.1016/j.epsl.2018.02.015

Yadava, M., Ramesh, R., & Pandarinath, K. (2007). A positive "amount effect" in the Sahayadri (western Ghats) rainfall. *Current Science*, *93*, 560–564.

Yoshimura, K., & Kanamitsu, M. (2008). Dynamical global downscaling of global reanalysis. *Monthly Weather Review*, *136*(8), 2983–2998. https://doi.org/10.1175/2008MWR2281.1

Yoshimura, K., Kanamitsu, M., Noone, D., & Oki, T. (2008). Historical isotope simulation using reanalysis atmospheric data. *Journal of Geophysical Research*, *113*, D19108. https://doi.org/10.1029/2008JD010074